J|A|C|S
ARTICLES
Published on Web 12/22/2001

Photoinduced Ultrafast Dye-to-Semiconductor Electron Injection from Nonthermalized and Thermalized Donor States

Gábor Benkö,[†] Jani Kallioinen,[‡] Jouko E. I. Korppi-Tommola,[‡] Arkady P. Yartsev,[†] and Villy Sundström*[,†]

Contribution from the Department of Chemical Physics, Lund University, P.O. Box 124, SE-22100 Lund, Sweden, and Department of Chemistry, University of Jyväskylä, P.O. Box 35, FIN-40351 Jyväskylä, Finland

Received July 9, 2001

Abstract: Electron injection from the transition metal complex $Ru(dcbpy)_2(NCS)_2$ (dcbpy = 4,4′-dicarboxy-2,2′-bipyridine) into a titanium dioxide nanocrystalline film occurs on the femto- and picosecond time scales. Here we show that the dominating part of the electron transfer proceeds extremely rapidly from the initially populated, vibronically nonthermalized, singlet excited state, prior to electronic and nuclear relaxation of the molecule. The results are especially relevant to the understanding and design of molecular-based photovoltaic devices and artificial photosynthetic assemblies.

Introduction

Understanding photoinduced electron transfer (ET) from transition metal complexes[1] into semiconductor thin films is important for the rational design and development of photovoltaic dye-sensitized devices, optical displays and sensors, photocatalytic processes, and artificial photosynthesis.[2,3] Since the first demonstration that light-induced electron injection occurs from $Ru(dcbpy)_2(NCS)_2$ (RuN3; dcbpy = 4,4′-dicarboxy-2,2′-bipyridine),[4] to the titanium dioxide film in Grätzel solar cells,[5,6] a key challenge has been to resolve and explain the mechanism of electron injection at the RuN3−TiO_2 interface.[7−12] A central issue, as hypothesized in some works,[7,9,12−14] is whether electron injection occurs before or after intramolecular energy relaxation processes (i.e., is the reaction nonergodic or ergodic?[15]) and how these processes influence the ET.

The ergodic limit,[15] a cornerstone in statistical theories of chemical reaction dynamics, implies strong coupling between intramolecular modes and the reaction occurs from a thermalized state. If a system is nonergodic, however, the reaction proceeds prior to energy equilibration over all the electronic, vibrational, and rotational degrees of freedom. Nonergodic behavior has been demonstrated for photodissociation reactions in a class of small organic molecules.[16] For other ultrafast reactions such as the photoisomerization of rhodopsin,[17] the photodissociation of CO from myoglobin,[18] and the electron injection in dye-sensitized TiO_2 films,[7−14,19] nonergodicity may also be important. In the latter case, if electron injection is indeed faster than intramolecular energy relaxation processes such as vibrational relaxation (IVR), internal conversion (IC), and intersystem crossing (ISC), then the excess vibronic energy of the photoexcited sensitizer molecule will be dissipated quickly into the semiconductor particle. In contrast, for injection slower than the intramolecular relaxation processes, the excess energy will be accumulated in the sensitizer. Thus, a nonergodic electron injection pathway in dye-sensitized TiO_2 implies the possibility of full utilization of the photon energy, whereas in the ergodic limit, energizing the sensitizer allows destructive side reactions that may influence the long-term stability of the system. Obviously, molecular complexes that undergo very fast ET are advantageous for, for example, the fabrication of solar cells that can work without loss of photovoltaic performance.

Interfacial ET in the RuN3-sensitized TiO_2 films has been the subject of intense research and a variety of electron injection rates were reported.[7−11] Most authors seem to agree on the presence of a sub-100 fs (1 fs = 10^{-15} s) component of the injection. In some works,[8,9] this ultrafast channel is considered

* Corresponding author: (e-mail) Villy.Sundstrom@chemphys.lu.se.
[†] Lund University.
[‡] University of Jyväskylä.

(1) Juris, A.; et al. *Coord. Chem. Rev.* **1988**, *84*, 85−277.
(2) Kalyanasundaram, K.; Grätzel, M. *Coord. Chem. Rev.* **1998**, *77*, 347−414.
(3) Bolton, J. R. *Sol. Energy Mater. Sol. Cells* **1995**, *38*, 543−554.
(4) Nazeeruddin, M. K.; et al. *J. Am. Chem. Soc.* **1993**, *115*, 6382−6390.
(5) O'Regan, B.; Grätzel, M. *Nature* **1991**, *353*, 737−739.
(6) Hagfeldt, A.; Grätzel, M. *Acc. Chem. Res.* **2000**, *33*, 269−277.
(7) Hannappel, T.; Burfeindt, B.; Storck, W.; Willig, F. *J. Phys. Chem. B* **1997**, *101*, 6799−6802.
(8) Asbury, J. B.; et al. *J. Phys. Chem. B* **1999**, *103*, 3110−3119.
(9) Tachibana, Y.; Moser, J. E.; Grätzel, M.; Klug, D. R.; Durrant, J. R. *J. Phys. Chem.* **1996**, *100*, 20056−20062.
(10) Tachibana, Y.; Haque, S. A.; Mercer, I. P.; Durrant, J. R.; Klug, D. R. *J. Phys. Chem. B* **2000**, *104*, 1198−1205.
(11) Kallioinen, J.; Lehtovuori, V.; Myllyperkiö, P.; Korppi-Tommola, J. *Chem. Phys. Lett.* **2001**, *340*, 217−221.
(12) Asbury, J. B.; et al. *J. Phys. Chem. B* **2001**, *105*, 4545−4557.
(13) Moser, J. E.; Grätzel, M. *Chimia* **1998**, *52*, 160−162.
(14) Ferrere, S.; Gregg, B. A., *J. Am. Chem. Soc.* **1998**, *120*, 843−844.
(15) For a general overview, see: Bernstein, R. B.; Zewail, A. H. *J. Phys. Chem.* **1986**, *90*, 3467−3469.
(16) Diau, E. W.-G.; Herek, J. L.; Kim, Z. H.; Zewail, A. H. *Science* **1998**, *279*, 847−850.
(17) Peteanu, L. A.; Schoenlein, R. W.; Wang, Q.; Mathies, R. A.; Shank, C. V. *Proc. Natl. Acad. Sci. U.S.A.* **1993**, *90*, 11762−11766.
(18) Owrutsky, J. C.; Li, M.; Locke, B.; Hochstrasser, R. M. *J. Phys. Chem.* **1995**, *99*, 4842−4846.
(19) Benkö, G.; Hilgendorff, M.; Yartsev, A. P.; Sundström, V. *J. Phys. Chem. B* **2001**, *105*, 967−974.

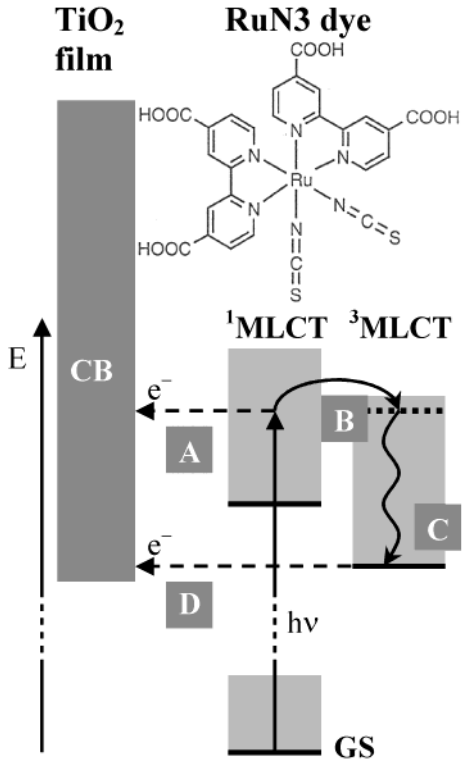

Figure 1. Schematic model for two-state electron injection and structure of RuN3. Following MLCT excitation (at 530 nm) of the RuN3-sensitized TiO_2 film, an electron is promoted from a mixed ruthenium-NCS state to an excited π^* state of the dcbpy ligand[4,6,8,21,22] and injected into the conduction band (CB) of the semiconductor. GS: ground state of RuN3. Channel A: electron injection from the nonthermalized, singlet ^{1}MLCT excited state. Channels B and C: ISC followed by internal vibrational relaxation in the triplet ^{3}MLCT excited state. Channel D: electron injection from the thermalized, triplet ^{3}MLCT excited state.

to be the only or dominant process. Other groups[9−11] have reported additional contributions of slower nonexponential electron injection with a distribution of characteristic times from 1 ps (1 ps = 10^{-12} s) to tens of picoseconds. The origin of this discrepancy is not clear. In addition to electron injection, the photoexcited dye molecule is known to undergo a number of ultrafast relaxation processes. For a similar transition metal complex ($[Ru(bpy)_3]^{2+}$) in solution or adsorbed to a nonreacting semiconductor surface, fast ISC and solvent-driven electron localization following metal-to-ligand charge transfer (MLCT) excitation has been demonstrated to occur with a time constant of ∼100 fs.[1,20,21] These processes are expected to occur in parallel with electron injection in the case of RuN3 adsorbed to TiO_2 films.

Previous time-resolved measurements of dye-to-semiconductor ET have been performed with a temporal resolution of ∼100 fs or longer, precluding differentiation of intramolecular relaxation processes of the sensitizer (such as ISC) from the ET reactions. In the present work, we have performed ultrafast transient absorption measurements with either improved temporal or spectral resolution that allow us to distinguish these processes and identify and characterize the pathways of ET from the RuN3 to the TiO_2. We will use the simplified energy level diagram of Figure 1 to discuss our results. The key feature of this model is electron injection from both the initially excited,

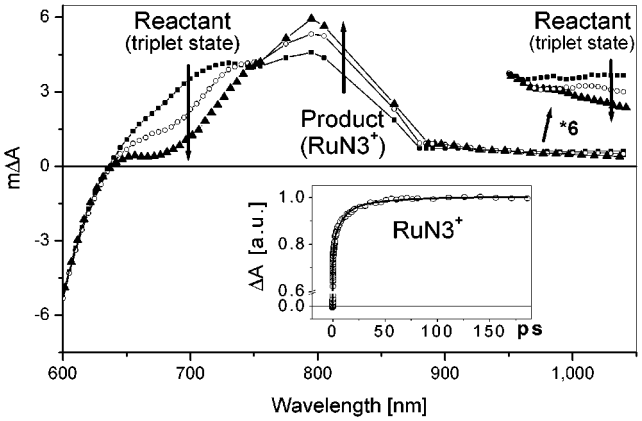

Figure 2. Visible and near-IR transient absorption spectra of RuN3-sensitized TiO_2 film. At time delays of 0.5 (■), 10 (○), and 150 ps (▲) between the pump and probe pulses, we observe characteristic dynamics of the differential spectra with two isobestic points (the wavelength where $\Delta A_{reactant} = \Delta A_{product}$) at 760 and 940 nm and one nearly time-independent $\Delta A = 0$ point at 630 nm. This type of spectral structure signifies a reactant-to-product transition and is further supported by the observed dynamics of the characteristic spectral bands: the identical decays of the "reactant"-related bands and the corresponding rise of the "product" band. Inset: transient absorption kinetics of oxidized RuN3 cation−TiO_2 measured at 860 nm. Symbols are measured data, while the curve is a fit with the following time constants and amplitudes: rise within the laser pulse (20 ± 5%), 28 ± 3 fs (50%), 1 ± 0.1 ps (11%), 9.5 ± 1 ps (12%), and 50 ± 5 ps (7%).

nonthermalized, singlet state of the dye (channel A of Figure 1) and the thermalized triplet state (channel D)—to account for the observed vastly different electron injection times ranging from ∼50 fs to ∼50 ps.

Results and Discussion

Electron Injection from the Triplet State of the Dye. We start by considering the results identifying ET from the triplet state (channel D of Figure 1). Figure 2 displays the transient absorption spectrum of RuN3-sensitized TiO_2 film at delay times longer than 0.5 ps, when the dye already has relaxed to its triplet state.[20,21]

By comparison of the recorded transients with previously reported spectra[9,20,23−26] and kinetics,[11] we can clearly determine the nature of the reactant and product as corresponding to triplet state and oxidized RuN3, respectively. The band at 690 nm and the weak and featureless band at longer wavelengths (>900 nm) monitor the decay of the triplet state. Both transitions are due to absorption from a ^{3}MLCT state, localized on the reduced dcbpy ligand of the dye.[9−11,23,24] The formation of the product, the oxidized RuN3 molecule ($RuN3^+$), is shown by the rise of absorption around 810 nm due to the NCS ligand-to-Ru^{3+} charge-transfer transition.[9−11,23,25,26] Due to overlap of the various signals in this spectral region, we could not detect the appearance of the other reaction product, the electrons in the conduction band of the semiconductor.[27] Their weak absorption[19,27] can however be seen after 150 ps (see Figure 2), when only the absorption of the conduction band electrons (∼630−

(20) Damrauer, N. H.; et al. *Science* **1997**, *275*, 54−57.
(21) Yeh, A. T.; Shank, C. V.; McCusker, J. K. *Science* **2000**, *289*, 935−938.
(22) Rensmo, H. thesis, Uppsala University, Sweden, 1998.
(23) Moser, J. E.; et al. *J. Phys. Chem. B* **1998**, *102*, 3649−3650.
(24) Damrauer, N. H.; McCusker, J. K. *J. Phys. Chem. A* **1999**, *103*, 8440−8446.
(25) Das, S.; Kamat, P. V. *J. Phys. Chem. B* **1998**, *102*, 8954−8957.
(26) Kuciauskas, D.; Freund, M. S.; Gray, H. B.; Winkler, J. R.; Lewis, N. S. *J. Phys. Chem. B* **2001**, *105*, 392−403.
(27) Rothenberger, G.; Fitzmaurice, D.; Grätzel, M. *J. Phys. Chem.* **1992**, *96*, 5983−5986.

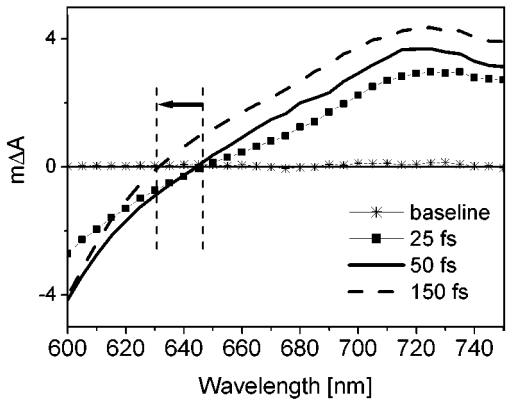

Figure 3. Femtosecond transient absorption spectra of RuN3-sensitized TiO_2 film in the wavelength region 600−750 nm at delay times from 25 to 150 fs. The arrow indicates the direction and magnitude of the blue-shift caused by the formation of the triplet state.

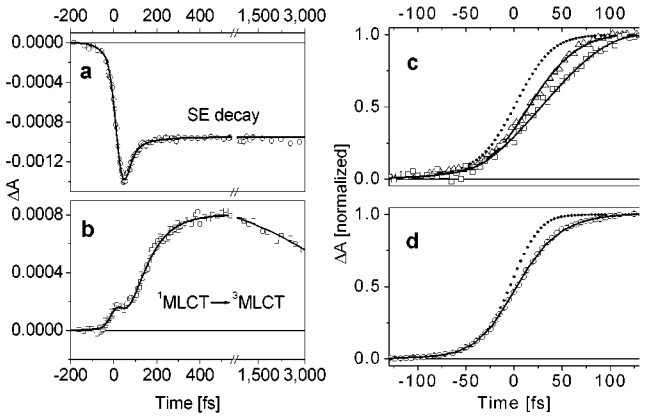

Figure 4. Transient absorption kinetics. Open symbols are measured data, curves are fits, and the instrument responses are represented by dotted curves. (a) SE decay probed at 600 nm; (b) excited-state evolution (^{1}MLCT → ^{3}MLCT) probed at 690 nm; (c) formation of the triplet state at 1050 nm. The data are well fitted with rise times of 30 ± 5 (for RuN3−TiO_2; triangles) and 70 ± 15 fs (for RuN3−EtOH; squares). (d) Early-time transient absorption kinetics of oxidized RuN3 cation−TiO_2 measured at 860 nm; parameters of the fit are given in the caption of Figure 2.

690 and ∼930−1050 nm) and oxidized dye (∼690−930 nm) is present. To quantify the time evolution of the observed spectral features, kinetics were measured in the three bands at different wavelengths between 640 and 1050 nm. The excellent agreement (the comparison is provided as Supporting Information) between the decay of the triplet state monitored at 690 and 1050 nm and rise of the oxidized dye measured at 770, 790, 810, and 860 nm (inset of Figure 2) implies that electron injection from the thermalized triplet state proceeds in a nonexponential fashion and can be described by multiexponential kinetics with the predominant time constants of ∼1, ∼10, and ∼50 ps. On the basis of the present study, we can rule out any ultrafast (≪1 ps) injection component from the triplet state. This could not be established from previous studies,[9−11] because only the time constants for the overall electron injection, ranging from less than 100 fs to tens of picoseconds, were reported.

Electron Injection from the Initially Excited Singlet State of the Dye. To distinguish the early-time involvement of the singlet channel in the ET, we used ∼30-fs laser pulses to monitor the optical population of the singlet state, and its decay into the triplet state intermediate and oxidized dye product (channels A−C of Figure 1). Already the transient spectra of Figure 3 measured with ∼100-fs resolution resolve the delayed appearance of the triplet state: since the formation of both the initial excited state and ground-state bleach is instantaneous,[9,10,20,24] the blue-shift of the transient spectra at around the $\Delta A = 0$ crossing point (∼645 nm) can be assigned to the formation of the triplet excited state during the first 150 fs. Taken alone, this spectral evolution is not sufficient to unambiguously identify the process responsible for these dynamics. However, by carefully comparing the kinetics at spectral positions corresponding to stimulated emission of the initially excited state and absorption from the triplet state and oxidized dye product, we show that the triplet state and oxidized dye are formed with a time constant of ∼30 fs from the initially excited state (see below).

To follow the time evolution of the initially prepared excited state in more detail, we recorded the dynamics of the excited-state absorption (ESA) and stimulated emission (SE) signals. It is natural to expect SE from the singlet state populated by light absorption. For $[Ru(bpy)_3]^{2+}$ in acetonitrile, spontaneous emission from the ^{1}MLCT state with ∼60-fs time constant has been measured recently by using femtosecond fluorescence upconversion.[28] However, for RuN3, singlet SE was not previously observed, as ISC in this molecule is very fast and efficient. In the present study, we succeeded in recording the decay of SE from the photoexcited ^{1}MLCT state by probing the sample at 600 nm. The measured kinetics (Figure 4a) show instantaneous formation of the negative signal followed by fast recovery with a time constant of ∼30 fs to a level that remains constant for more than 3 ps. The SE signal does not return to zero on the picosecond time scale because of the residual ground-state bleach that is present at these time delays at ∼600 nm. Other possible assignments of this signal can be eliminated. Ground-state recovery by a very fast radiationless internal conversion from the excited state to the ground state or electron injection followed by immediate recombination is excluded on the basis of the close to unity quantum yield of the light-induced ET and very slow recombination in the RuN3−TiO_2 system.[2,6,9,10] A transient increase of induced absorption from the triplet state or ET products (oxidized RuN3 or conduction band electrons) is also not feasible because these species have negligible extinction coefficients at this wavelength that cannot account for the amplitude of the fast decay.[23,27] Moreover, from the data of Figures 2 and 4b (see below), we know that the dynamics of the triplet state and ET products are associated with kinetics on the subpicosecond and picosecond time scale in contrast to the recorded time-independent response at 600 nm in the time interval ∼100 fs−3 ps (Figure 4a). Since the SE decay signal was recorded with parallel polarized pump and probe pulses, it might be susceptible not only to population decay in the excited state but also to an ultrafast change in the direction of the transition dipole moment that can be caused, for example, by electron localization driven by a solvation process following photoinduced charge transfer.[21] Such a process can be excluded in the present study because it was shown to take place on different time scale, ∼60 fs.[21] Depolarization effect in our study would be further decreased as the RuN3 excited-state population decays mainly as a result of electron injection before electron localization takes place (see below).

(28) Bhasikuttan, A. C.; Suzuki, M.; Nakashima, S.; Okada, T. *XX International Conference on Photochemistry*, Moscow, 2001; Abstract PP29.

Ultrafast dynamics matching the decay of the singlet state can also be observed in other spectral regions. At 690 nm (Figure 4b), the instantaneous rise followed by the 30 ± 3 fs decay again reflects the evolution of the singlet state, while the 80 ± 5 fs rise corresponds to the formation and thermalization of the triplet state (channels B and C of Figure 1). It is intriguing that the decay of the singlet proceeds in ~30 fs, but the rise of the triplet state occurs in ~100 fs. However, the probe signal centered at 690 nm in the blue wing of the triplet absorption band[9,10,23] (Figure 2) is sensitive to the spectral blue-shift caused by the triplet equilibration process. Thus, the ~100-fs time constant encompasses both the ISC process and ensuing thermalization of the triplet state. The kinetics at 1050 nm (Figure 4c) provide one more possibility to monitor the formation of the triplet state. In this spectral region, the absorption of the triplet is very broad and featureless and therefore not sensitive to spectral shifts that may be caused by the thermalization processes. Hence, a ~30-fs rise time is observed, corresponding directly to the decay of the singlet state monitored by SE. In Figure 4c, the formation of the triplet state for RuN3 in solution is compared to that of RuN3-sensitized TiO_2 film and found to be considerably slower in solution (~70 fs). The faster formation of the triplet in RuN3−TiO_2 likely reflects the very fast and efficient electron injection from the singlet state prior to IVR, IC, and ISC (see below). Finally, if the ~30-fs decay corresponds to electron injection from the RuN3 singlet state, then we expect to observe this time constant also for the formation of the oxidized RuN3. Indeed, the fit to the data at 860 nm (Figure 4d) confirms the presence of the ~30-fs time constant with high amplitude (>50%). Hence, we see that the optically excited singlet state decays with the same time constant of ~30 fs as the triplet state and oxidized dye products appear, thus coupling these species in a reactant−product relationship.

In a simplified reaction model, the rate constant related to the observed ~30-fs decay of the singlet state reflects the sum of the rates of electron injection from the ^{1}MLCT state (k_A) and ISC (k_B): $^1/_{30}$ fs^{-1} = $k_A + k_B$. The ratio between k_A and k_B of 1.5 is calculated from the amplitude ratio of femtosecond (~60%) and picosecond (~40%) electron injection contributions to the signal at 860 nm. The equation yields $k_A = {}^1/_{50}$ fs^{-1} and $k_B = {}^1/_{75}$ fs^{-1}. The value determined for $1/k_B$ is in good agreement with previous measurements of ISC for this class of molecules[8,20,21] and is in excellent agreement with the formation of the triplet state measured here for RuN3 in ethanol solution. We conclude that, after excitation of the sample at 530 nm, ~60% of the RuN3 molecules inject electrons from the singlet state into TiO_2 (channel A of Figure 1) and the rest undergoes ISC (channel B). After relaxation to the bottom of the triplet state (channel C), electrons are again injected into the semiconductor but now the reaction occurs on the picosecond time scale (channel D). It should be noted that our simplified model does not account for the distribution of vibrational levels in the singlet state populated by the spectrally broad laser pulse and for the possibly different rates of electron injection from the different vibrational levels within the singlet and triplet manifolds. Thus, we expect that in our experiments only an average of electron injection is observed for a certain center wavelength of excitation. The rapid formation of the triplet state suggests fast motion of the excitation wave packet away from the singlet state without significant evolution on the initial surface, similar to what has been suggested in other work.[7,20] As a result, the fast part of electron injection occurs from the nonthermalized singlet state strongly competing with excited-state relaxation processes (see below, also the discussion for 455-nm excitation). Further support of ET from the nonthermalized state may come from our observations of periodic oscillations in the kinetics of the RuN3$^+$, similar to what was observed in ref 29. The frequencies of the oscillations can be correlated to the Raman modes of the $[Ru(bpy)_3]^{2+}$.[30] This shows that vibrational coherence persists on a time scale long compared to singlet electron injection. According to a new theoretical model,[29,31] modulation of the ET by a vibrational wave packet directly shows that electron injection proceeds from a nonthermalized vibrational state. Presentation of the data is beyond the scope of the present paper and will be published elsewhere.[32]

Regarding the dramatic difference in injection times from singlet and triplet states, we suggest two factors that may influence the rate of interfacial ET. First, the increase of the density of acceptor states in TiO_2 above the edge of the conduction band results in more energy levels available to the singlet excited RuN3 molecule, thereby speeding up ET. The other factor is related to the different electronic nature of singlet and triplet states in RuN3, resulting in different couplings between the energy levels of the excited donor molecule and acceptor semiconductor particle.

Experimental evidence supporting the density-of-states argument was obtained by measuring the rates of ET as a function of the excitation wavelength. When the RuN3-sensitized TiO_2 film is excited with pulses of central wavelength at 455 nm and the formation of the oxidized dye probed at 860 nm, the kinetics are again highly nonexponential (data not shown). The best fit required a multiexponential rise with the following time constants and amplitudes: pulse-width-limited rise (70 ± 5%), 1.8 ± 0.2 (15%), 10 ± 1 (3%), and 50 ± 5 ps (12%). Compared to the kinetics obtained with 530-nm excitation, in which most of the femtosecond rise component was resolved, in this case, ~70% of the rise amplitude occurs within the resolution of the spectrometer. This experimental finding indicates an upper limit of ~20 fs for the time scale of singlet electron injection when the sample is excited by 455-nm light. To the best of our knowledge, the known time scale of IVR extends from tens of femtoseconds to tens of picoseconds,[33] which implies that the femtosecond ET either precedes or occurs in concert with IVR in our system. We conclude that the kinetics of electron injection from RuN3 to TiO_2 are indeed dependent on the initially populated vibronic hot state: the higher the state, the faster the electron injection. This result implies that dyes with an excited-state redox potential below the conduction band edge of the semiconductor are also capable of electron injection—when they are excited by sufficiently energetic photons.[13,14]

(29) Zimmermann, C.; et al. *J. Phys. Chem. B* **2001**, *105*, 9245−9253.
(30) Webb, M. A.; Knorr, F. J.; McHale, J. L. *J. Raman Spectrosc.* **2001**, *32*, 481−485.
(31) Ramakrishna, S.; Willig, F. *J. Phys. Chem. B* **2000**, *104*, 68−77.
(32) Benkö, G.; Kallioinen, J.; Korppi-Tommola, J. E.; Yartsev, A. P.; Sundström, V., manuscript in preparation.
(33) For example, for *trans*-stilbene, see: (a) Kolvalenko, S. A.; Schanz, R.; Hennig, H.; Ernsting, N. P. *J. Chem. Phys.* **2001**, *115*, 3256−3273. (b) Nakabayashi, T.; Okamoto, H.; Tasumi, M. *J. Phys. Chem. A* **1998**, *102*, 9686−9695. (c) Baskin, J. S.; Banares, L.; Pedersen, S.; Zewail, A. H. *J. Phys. Chem.* **1996**, *100*, 11920−11933 and references therein.

Conclusions

By examining interfacial ET in a transition metal complex/semiconductor system, this work provides an example of a chemical reaction whose value for practical applications largely relies on the fact that it occurs in the nonergodic regime of reaction dynamics. Our findings open the door to future designs of materials for optimal conversion of light energy to electrical energy and minimization of destructive photochemical side reactions, by demonstrating how the light energy absorbed by the sensitizer efficiently can be channelled into the energy of spatially separated charges prior to the onset of intramolecular relaxation processes.

Experimental Section

Femtosecond Spectrometers. Time-resolved differential absorption measurements were conducted in the conventional manner. For measurements of transient absorption spectra, a 5-kHz amplified Ti:sapphire laser/collinear optical parametric amplifier system was used to generate excitation (530 nm) and probe pulses of the order of ∼100 fs. For probe and reference beam generation (white light continuum in a sapphire plate), a small portion of the laser output was used. Each spectral window was selected by a monochromator (resolution 5 nm) positioned after the sample. Compensation for group velocity dispersion was performed by properly shifting the delay line to keep the pump−probe delay time fixed for each wavelength. For transient absorption kinetic measurements, a 1-kHz amplified Ti:sapphire laser system with higher time resolution was used. Excitation (530 nm) and probe pulses of the order of ∼30 fs were generated by noncollinear optical parametric amplifiers (NOPA). For all measurements, the intensities of the probe, reference, and pump beams were measured by Si photodiodes. With proper software selection of the pulses, absorption changes as low as 10^{-5} could be recorded accurately. The polarization of pump and probe beams was kept parallel. The excitation pulse intensity of $\sim 10^{14}$ photon/cm^2 used was far from the saturation limit considering the optical cross section of the dye to be 5×10^{-17} cm^{-2}. The accurate zero-time delay at all probe wavelengths was determined by sum-frequency cross-correlation and by the nonresonant, low-amplitude "spike signal" in a ∼60-μm glass slide. All experiments were conducted at room temperature. Multiexponential analysis was used to quantify the recorded kinetics. Measured kinetics were analyzed with the deconvolution software Spectra Solve 2.01, Lastek Pty. Ltd. (1997).

RuN3-Sensitized TiO_2 Film. RuN3 dye and TiO_2 paste (average particle size in colloidal solution ∼9 nm) were purchased from Solaronix SA. To obtain a porous film of a uniform thickness of ∼1 μm, the following procedure was used: ∼10 μL/cm^2 paste was spread on a 0.06−0.08-mm-thick microscope cover slip, using Scotch Magic tape as the frame. After drying, the film was sintered at ∼430 °C for 10 min. When the film was cooled to ∼80 °C, it was placed for several hours in a RuN3−ethanol solution (concentration 3×10^{-4} M). The nonadsorbed dye was washed off by purging the film with ethanol. The film was dried at room temperature for 20−30 s, covered by CH_3-CN and another microscope cover slip, and sealed. The absorbance of the highly transparent dye-sensitized film was 0.45 ± 0.02 at 540 nm. The samples were prepared immediately prior to measurements. No degradation or modification of the sample was observed in steady-state spectra recorded before and after the pump−probe measurements.

Acknowledgment. We thank Dr. J. L. Herek for helpful discussions and critical reading of the manuscript. This research was funded by grants form the Delegationen för Energiförsörjning i Sydsverige (DESS), the Swedish Natural Science Research Council, the Knut and Alice Wallenberg Foundation, the Crafoord Foundation, the Trygger Foundation, European Science Foundation, the Academy of Finland (MATRA program, contract 40416), Graduate School Laskemo, and the European Community (contract HPRI-CT-1999-00041). We thank Prof. Dr. E. Riedle for making available to us the NOPA used to generate the ultrashort ∼30-fs pulses.

Supporting Information Available: Kinetics of the time evolution of the spectral features. This material is available free of charge via the Internet at http://pubs.acs.org.

JA016561N